

Experimental section

Physical measurements and instrumentation

¹H NMR spectra were recorded on a Bruker DPX 400 FT–NMR spectrometer 400 MHz at 298 K. Electrospray ionization mass spectra (ESI–MS) were performed on a Bruker Maxis 4G ESI–Q–TOF Bruker using electrospray ionization (positive ion mode: ESI) in CHCl₃ or MeCN solution. Elemental analyses of the complexes were made using a PerkinElmer 240 elemental analyzer. Electronic absorption spectra in the UV–visible region were recorded with a Shimadzu UV–3600 spectrophotometer, in a 10×1 mm or 10×10 mm quartz cell. The photoluminescence spectra were measured on Edinburgh Instruments FS 5 and FLS 980 fluorescence spectrophotometers. Time-dependent single-photon counting technology (picosecond to microsecond) and multi-channel scanning technology (microsecond to second) were used for decay lifetime acquisition, using FLS 980 fluorescence spectrophotometer with 405 nm laser light source. The quantum yields (QYs) were measured using a Hamamatsu C9920-02G absolute photoluminescence quantum yield (PLQY) measurement system. Scanning electron microscopy (SEM) experiments were performed by using field emission scanning electron microscope (FESEM, Hitachi, SU8010) operating at an electron acceleration energy of 1 kV and 10 μA. The SEM samples were prepared by dropcasting solutions onto a silicon wafer and dried naturally. Powder XRD was performed on a Rigaku X-ray diffractometer (D/max-rA, Cu–Kα radiation ($\lambda = 1.542 \text{ \AA}$)).

Crystal structure determination

Single-crystal diffraction data of platinum(II) complexes **1–4** were collected on a

Rigaku SuperNova X-ray diffractometer using micro-focus dual with X-ray Source of Cu-K α radiation ($\lambda = 1.54178 \text{ \AA}$) at 150 K. Using Olex2^{1, 2}, the structures were solved by SHELXT and refined using the full-matrix least-squares procedures within the SHELXTL software package. CCDC **2051570**, **2051571**, **2051572** and **2051573** contain the supplementary crystallographic data for complexes **1–4**, respectively, and can be obtained free of charge from the Cambridge Crystallographic Data Centre *via* www.ccdc.cam.ac.uk/data_request/cif.

Computational Details.

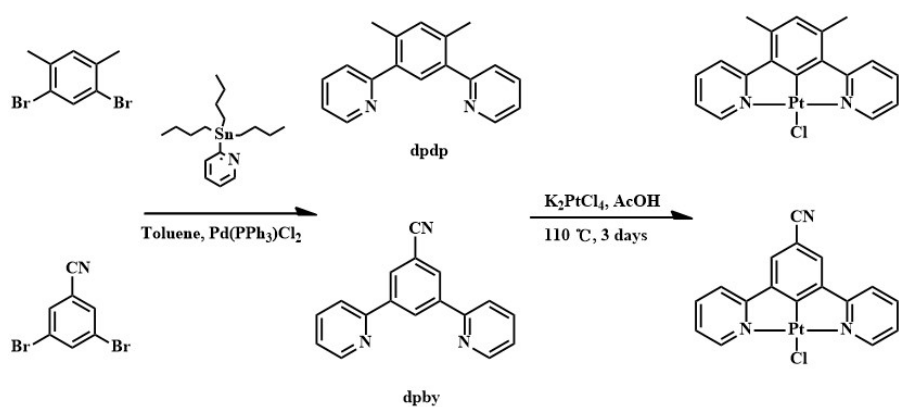
All the calculations are performed using combination of B3LYP/8–8G* (GENECP for Pt atoms) with the Gaussian 09 program suite.³ By density functional theory (DFT), the ground -state geometries of complexes **1–4** are fully optimized. Time-dependent DFT (TDDFT) calculations are then performed on the optimized ground-state geometries at the same level of theory to compute the singlet–singlet and singlet–triplet transitions. In order to gain more insight into the emissive states, the geometries of the lowest-lying triplet excited states (T_1) are optimized with unrestricted formalism.⁴

Fabrication of LED Devices

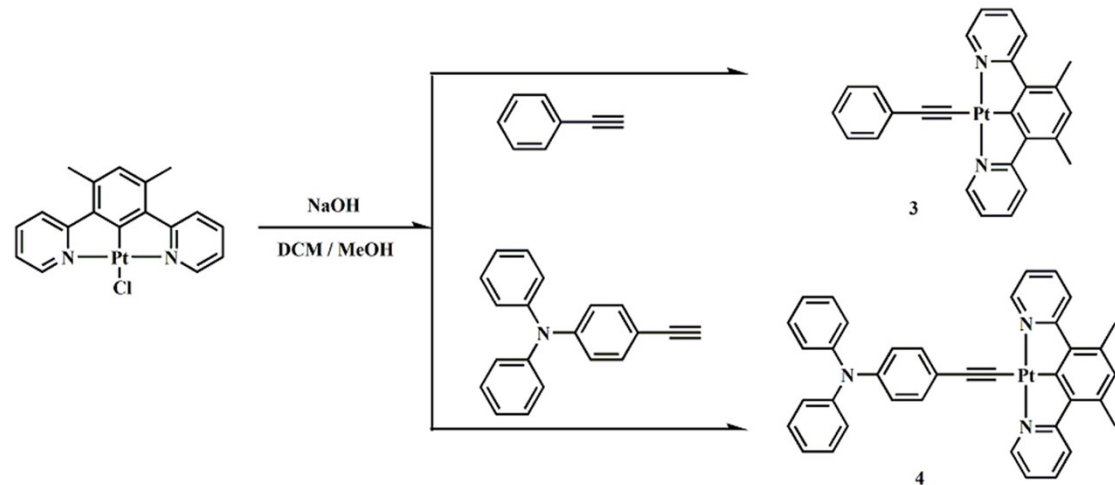
Putting 5 mg platinum(II) complexes **1–4** mixed with stoichiometric pouring sealant (HN3153–TCA/B) respectively, in a small beaker according to the mass ratio of 1:100, and then stirred thoroughly for 15 min. After deaeration in vacuum, the mixture was dropped on top of the commercial LED chip (an emission wavelength of about 380 nm) with possibly 2 mm thick films. The Electroluminescence measurements of LEDs were carried out at room temperature using the Photoresearch Spectrascan ® PR-735.

Materials and reagent

All starting materials were obtained from commercial suppliers and were used as received. The potassium tetrachloroplatinate(II) ($K_2[PtCl_4]$) were purchased from J&K Scientific Ltd. 2-(Tributylstanny)pyridine, *N*-(4-ethynylphenyl)-*N*-phenylbenzenamine, 1-ethynylbenzene and 1,5-dibromo-2,4-dimethylbenzene were obtained from the Aladdin Industrial Co. The chloroplatinum(II) complex precursor ($[Pt(N^C^N)Cl]$) was synthesized according to the literature⁵⁻⁸. The synthetic routes of chloroplatinum(II) complexes and target complexes **1-4** are shown in **Schemes S1** and **S2**, respectively.



Scheme S1 Synthetic routes of dpdp, dpby ligands, and platinum(II) complexes **1**, **2**.



Scheme S2 Synthetic routes of platinum(II) complexes **3** and **4**.

For **dpdP**: C₁₈H₁₆N₂: ¹H NMR (400 MHz, CDCl₃): δ 8.67 (s, 2H, –Py¹), 7.72 (m, 2H, –Py³), 7.45 (m, 3H, –Py⁴ and –Ph⁷), 7.21 (m, 3H, –Py² and –Ph⁶), 2.41 (s, 6H, –CH₃⁵). MS (ESI⁺): m/z : 261.13 (100%). Elemental analysis calcd (%) for C₁₈H₁₆N₂: C 83.04, H 6.19, N 10.76; found: C 83.06, H 6.21, N 10.72.

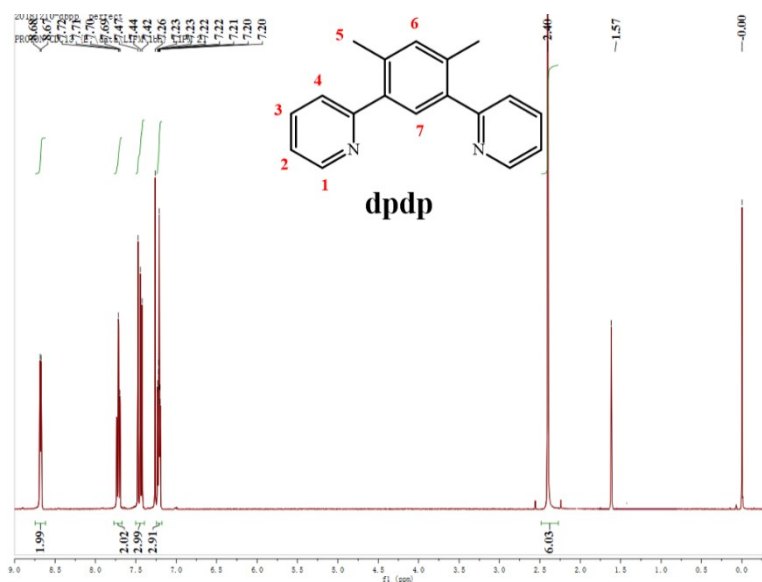


Figure S1 ¹H–NMR spectra for ligand **dpdP**.

For **dpby**: C₁₇H₁₁N₃: ¹H NMR (400 MHz, CDCl₃): δ 8.91 (s, 1H, -Ph¹), 8.78 (d, 2H, -Py²), 8.39 (d, 2H, -Ph⁶), 7.86 (m, 4H, -Py^{3, 4}), 7.36 (m, 2H, -Py⁵). MS (ESI⁺): m/z : 258.29 (100%). Elemental analysis calcd (%) for C₁₇H₁₁N₃: C 79.36, H 4.31, N 16.33; found: C 79.29, H 4.34, N 16.35.

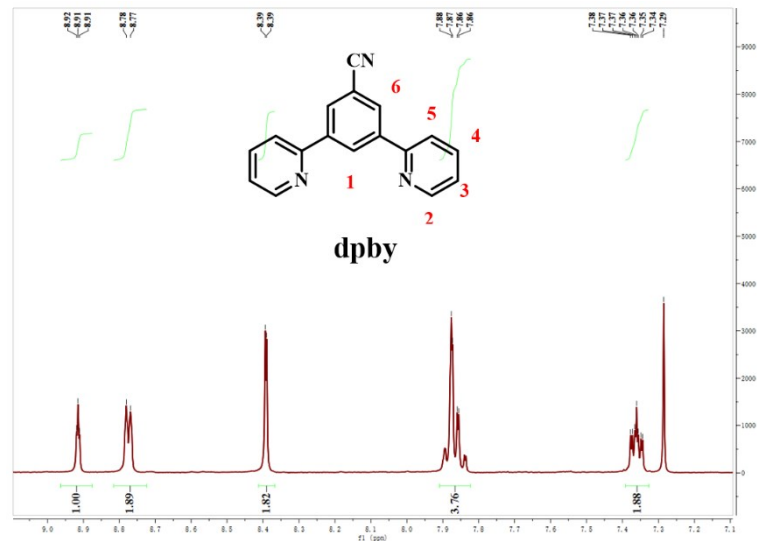


Figure S2 ^1H -NMR spectra for ligand **dpby**.

For **1**: C₁₈H₁₅N₂ClPt: ¹H NMR (400 MHz, CDCl₃): δ 9.48 (m, 2H, -Py¹), 7.86 (m, 4H, -Py^{2, 4}), 7.21 (t, 2H, -Py³), 6.78 (s, 1H, -Ph⁵), 2.65 (s, 6H, -CH³). MS (ESI⁺): m/z: 454.09 [M–Cl]⁺. Elemental analysis calcd (%) for C₁₈H₁₅N₂ClPt: C 47.58, H 3.33, N 6.16; found: C 47.53, H 3.29, N 6.19.

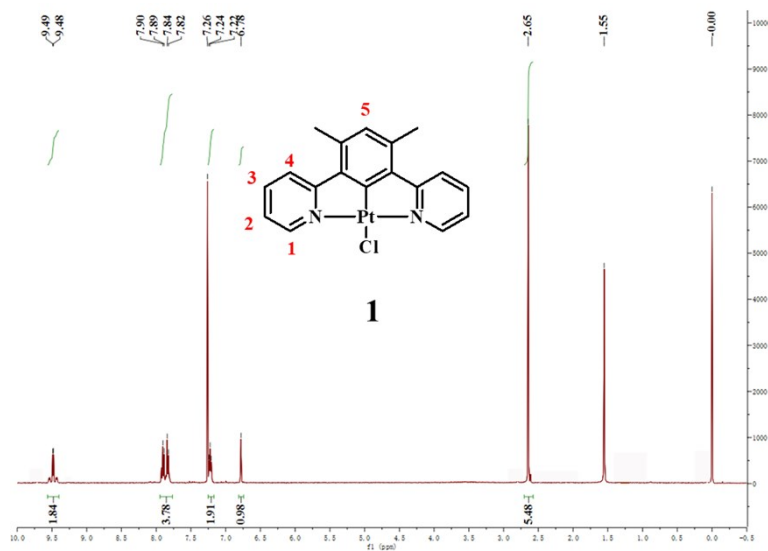


Figure S3 ¹H-NMR spectra of complex **1**

For **2**: C₁₇H₁₀N₃ClPt: ¹H NMR (400 MHz, d–DMSO): δ 9.16 (d, 2H, –Py¹), 8.29 (m, 6H, –Py^{2,3} and –Ph⁵), 9.15 (m, 2H, –Py⁴). MS (ESI⁺): m/z: 452.37 [M–Cl]⁺. Elemental analysis calcd (%) for C₁₇H₁₀N₃ClPt: C 41.94, H 2.07, N 8.63; found: C 41.96, H 2.03, N 8.66.

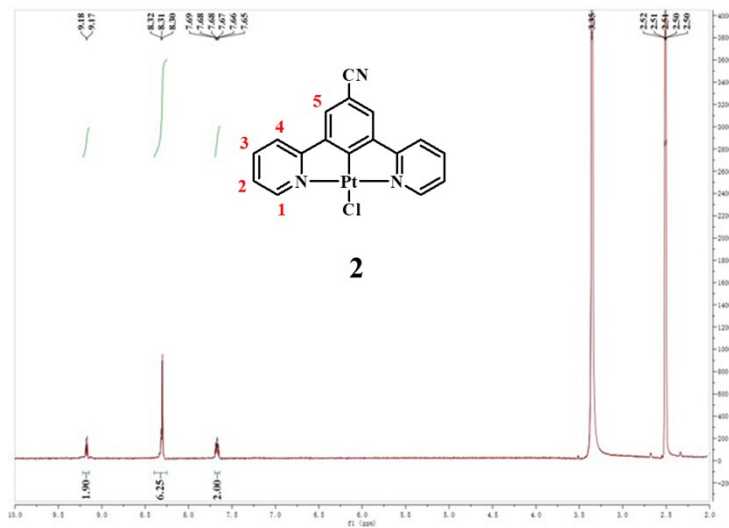


Figure S4 ¹H–NMR spectra of complex **2**.

For **3**: C₂₆H₂₀N₂Pt: ¹H NMR (400 MHz, CDCl₃): δ 9.66 (d, 2H, -Py¹), 7.88 (m, 4H, -Py^{2,4}), 7.58 (t, 2H, -Ph⁶), 7.30 (d, 2H, -Ph⁷), 7.19 (m, 3H, -Ph^{3,8}), 2.65 (s, 6H, -CH³). MS (ESI⁺): m/z: 555.13. Elemental analysis calcd (%) for C₂₆H₂₀N₂Pt: C 56.21, H 3.23, N 5.04; found: C 56.24, H 3.19, N 5.06.

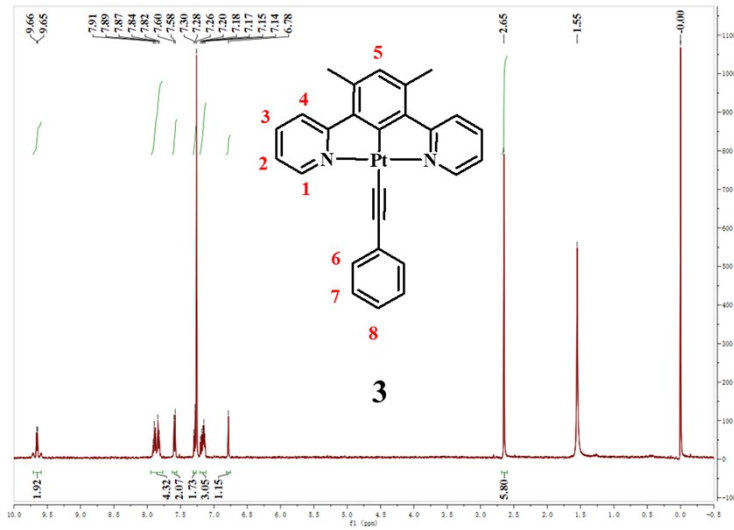


Figure S5 ¹H–NMR spectra of complex **3**.

For **4**: C₃₈H₉N₃Pt: ¹H NMR (400 MHz, CDCl₃): δ 9.65 (s, 2H, -Py⁵), 7.89(t, 2H, -Py³), 7.83 (d, 2H, -Py²), 7.48 (d, 2H, -Ph⁶), 7.23 (d, 4H, -Ph^{9, 11}), 7.12 (m, 6H, -Ph^{7, 8, 12}), 7.00 (m, 4H, -Py⁴ and -Ph¹⁰), 6.78 (s, 1H, -Ph¹), 2.65 (s, 6H, -CH₃). MS (ESI⁺): m/z: 723.74. Elemental analysis calcd (%) for C₃₈H₉N₃Pt: C 63.15, H 4.04, N 5.81; found: C 63.06, H 4.15, N 5.79.

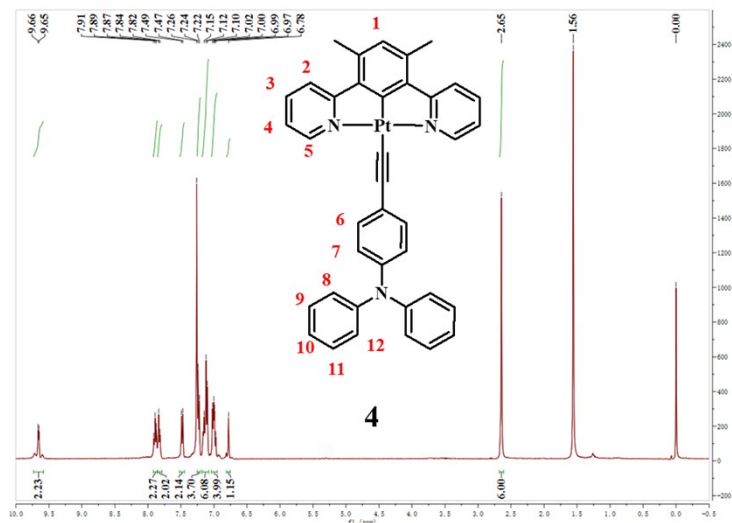


Figure S6 ¹H–NMR spectra of complex **4**.

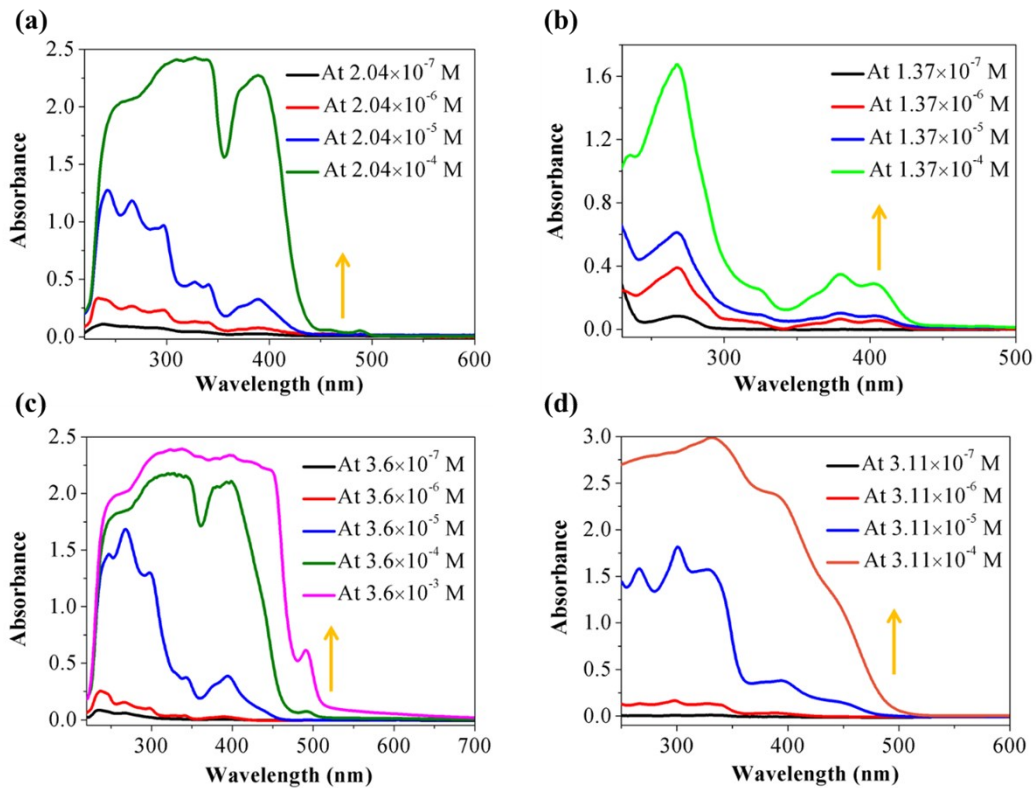


Figure S7 Concentration dependent UV–vis absorption spectra of the complexes a), 1; b), 2; c), 3; d), 4.

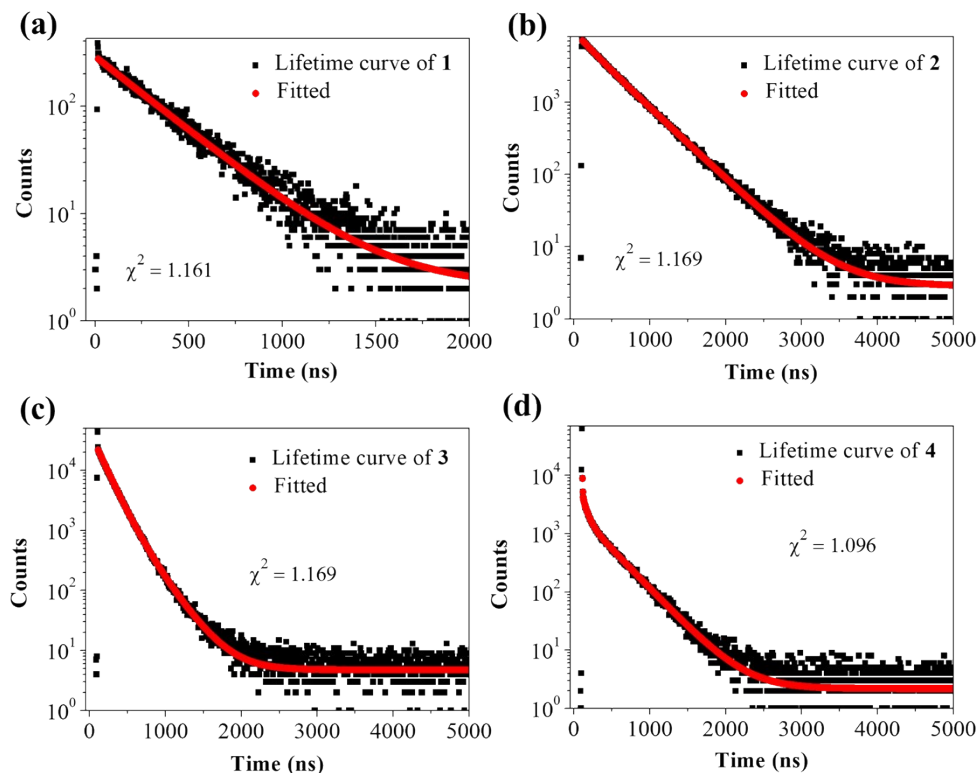


Figure S8 Decay curves of complexes 1–4 in DCM solution at room temperature.

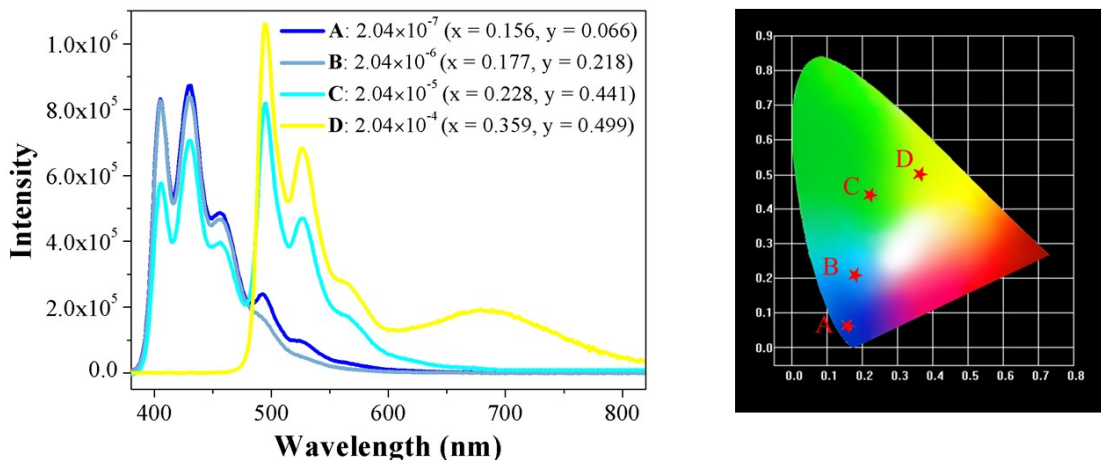


Figure S9 Concentration dependent emission spectra of complex **1**.

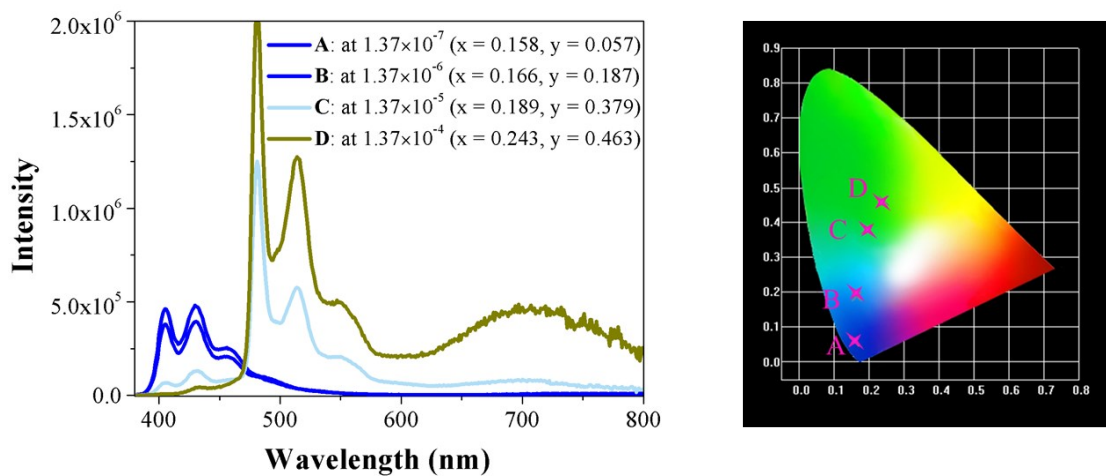


Figure S10 Concentration dependent emission spectra of complex **2**.

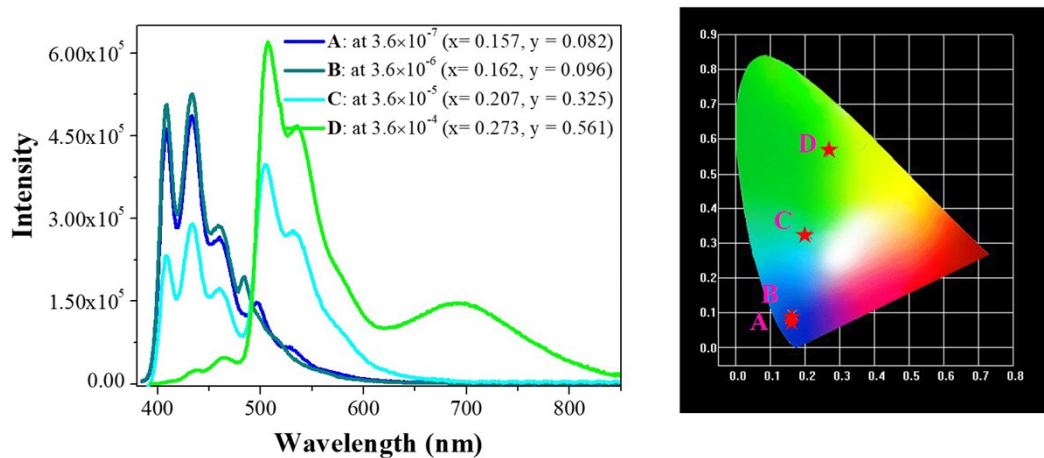


Figure S11 Concentration dependent emission spectra of complex **3**.

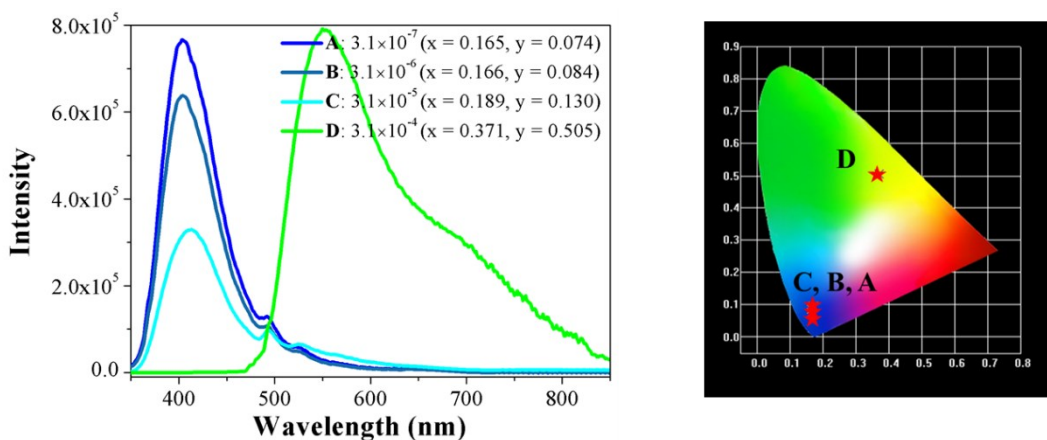


Figure S12 Concentration dependent emission spectra of complex **4**.

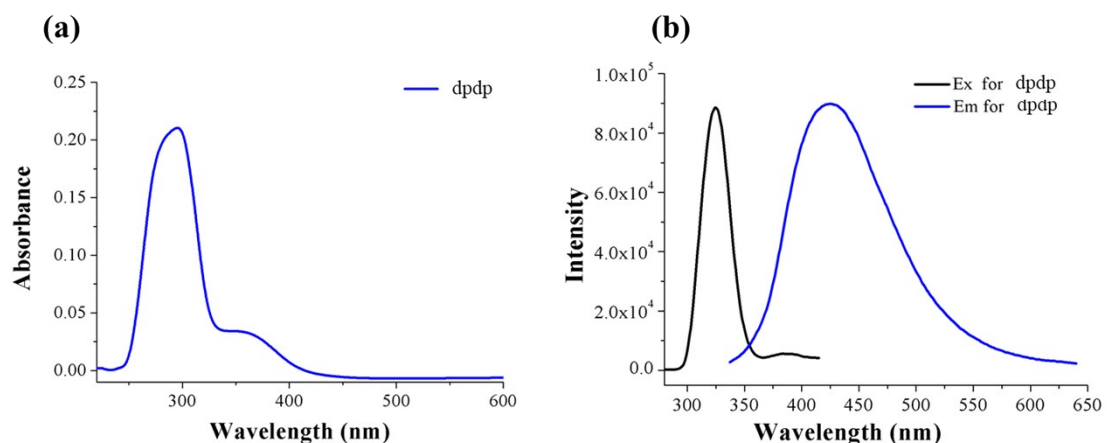


Figure S13 UV–vis absorption (a), and excitation, emission (b) spectra of the ligand dpdp at the concentration of 10⁻⁵ M at RT.

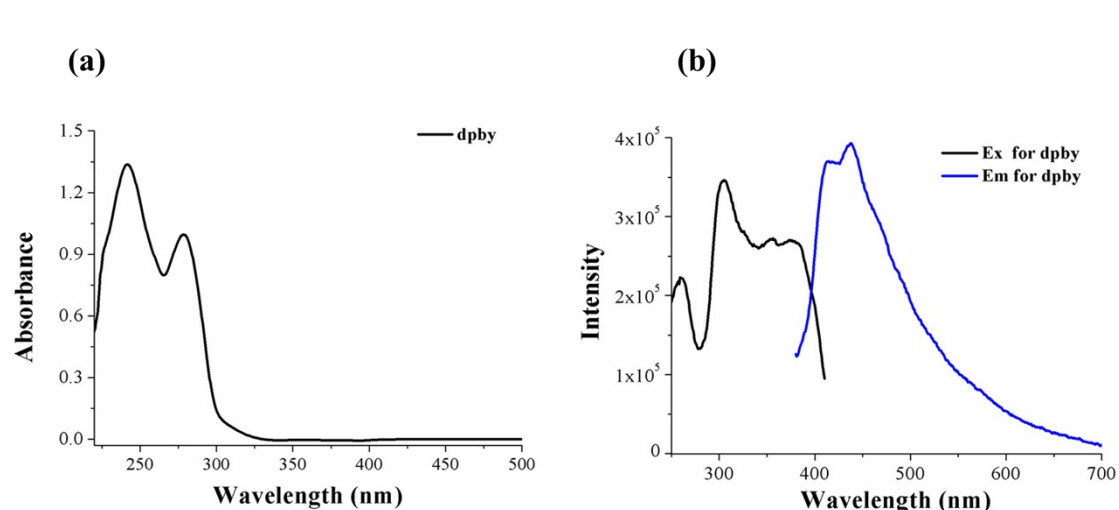


Figure S14 UV–vis absorption (a), and excitation, emission (b) spectra of the ligand dpby at the concentration of 10⁻⁵ M at RT.

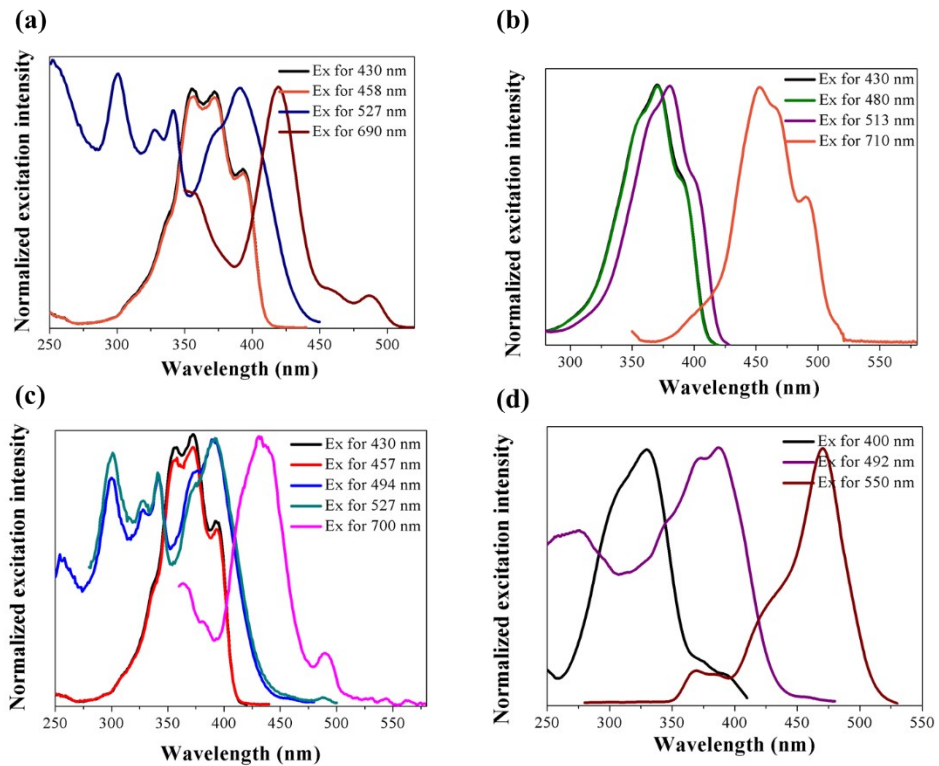


Figure S15 Normalized excitation spectra at different emission wavelengths of complexes **1–4** in DCM solution, a) **1**, b) **2**, c) **3** and d) **4**.

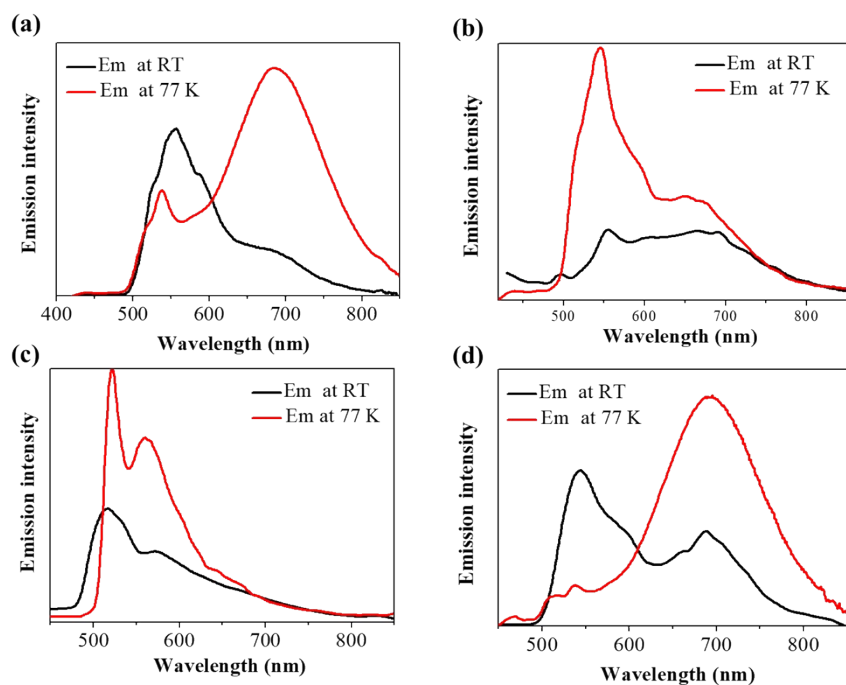


Figure S16 Normalized emission spectra of complexes **1–4** in solid state at 77 K and room temperature (RT), a) **1**, b) **2**, c) **3** and d) **4**.

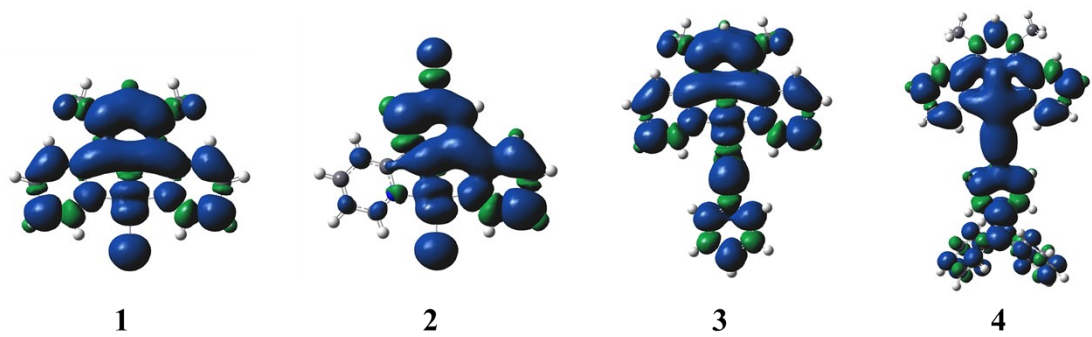


Figure S17 Spin density of T_1 states of **1–4**.

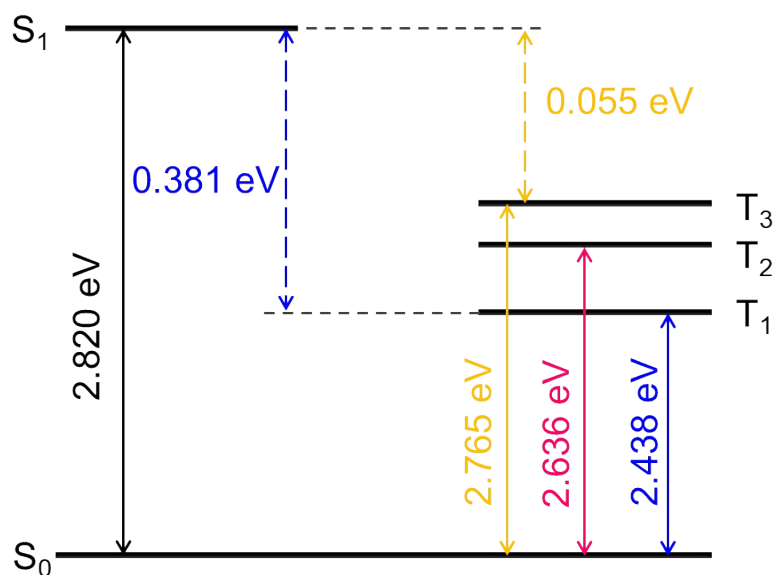


Figure S18 Orbital energy diagram of complex **1**.

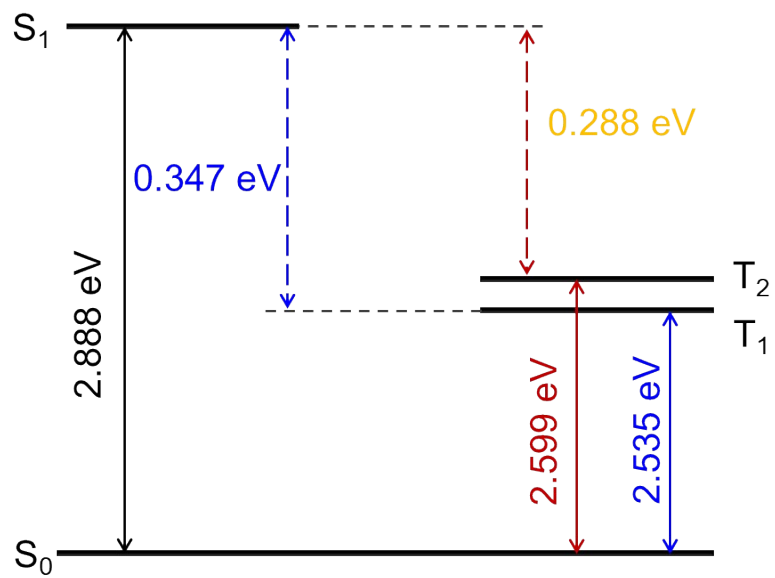


Figure S19 Orbital energy diagram of complex 2.

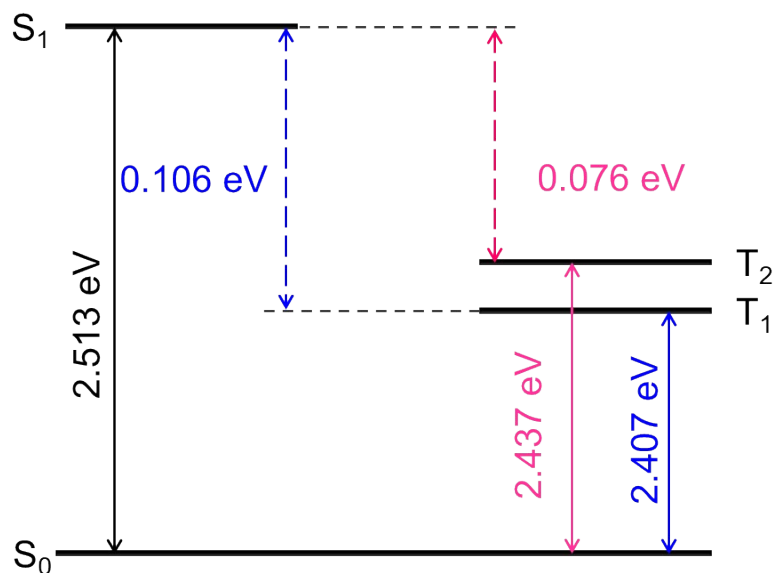


Figure S20 Orbital energy diagram of complex 3.

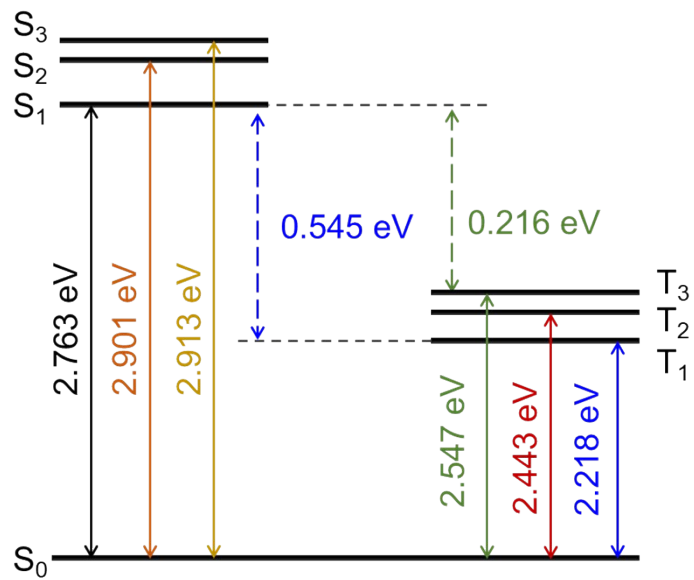


Figure S21 Orbital energy diagram of complex 4.

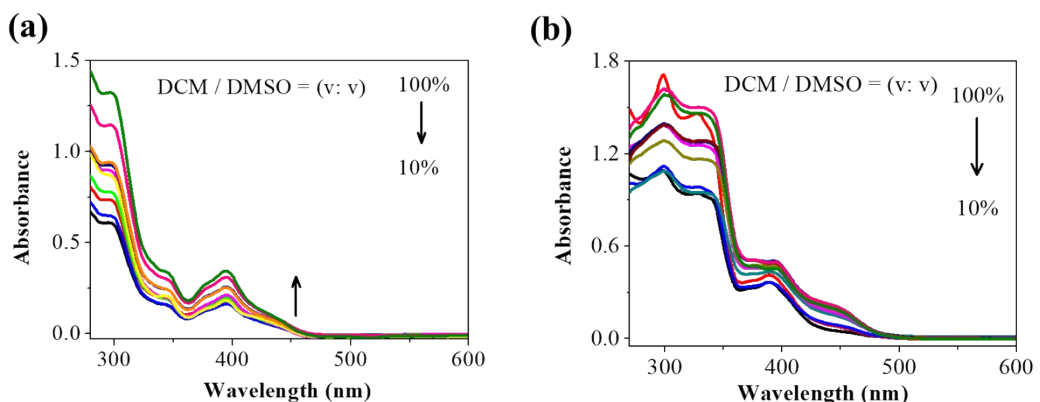


Figure S22 UV-vis absorption spectra of **3** (a) and **4** (b) (10^{-6} M) upon increasing the DMSO content in DCM with the ratio of 0% to 90 %.

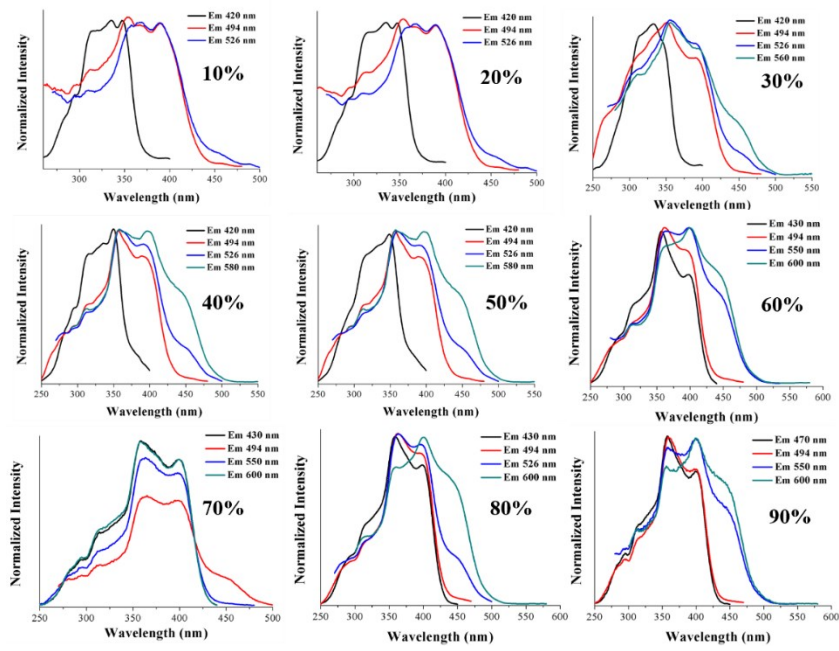


Figure S23 Normalized excitation spectra of complex 4 under the different ratio of DCM/DMSO (10%–90%) at the concentration of 10^{-5} M.

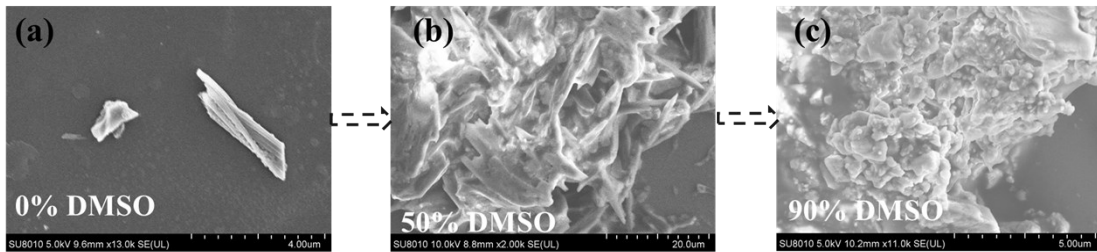


Figure S24 SEM images of complex 3 in DCM/DMSO mixture solutions (0%, 50% and 90% DMSO, respectively).

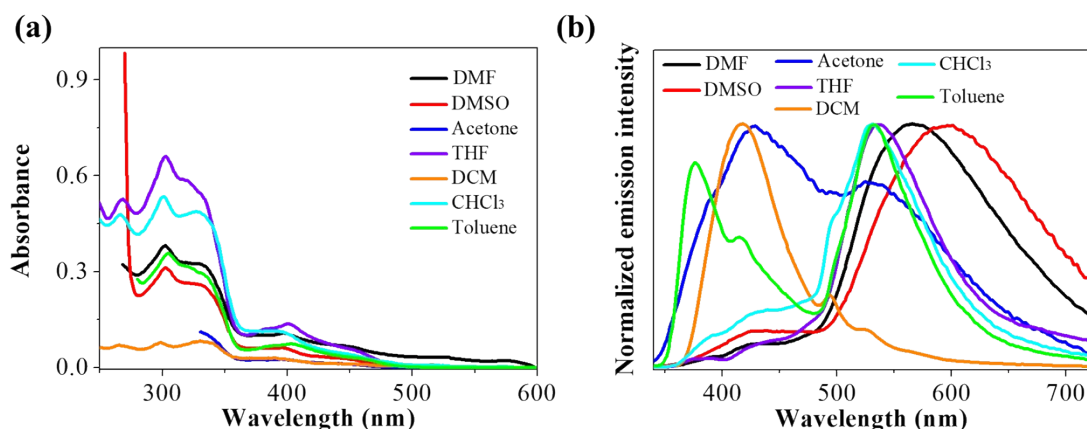


Figure S25 (a) UV–vis absorption and (b) normalized emission spectra of complex 4 in different solvents (10^{-6} M) at room temperature.

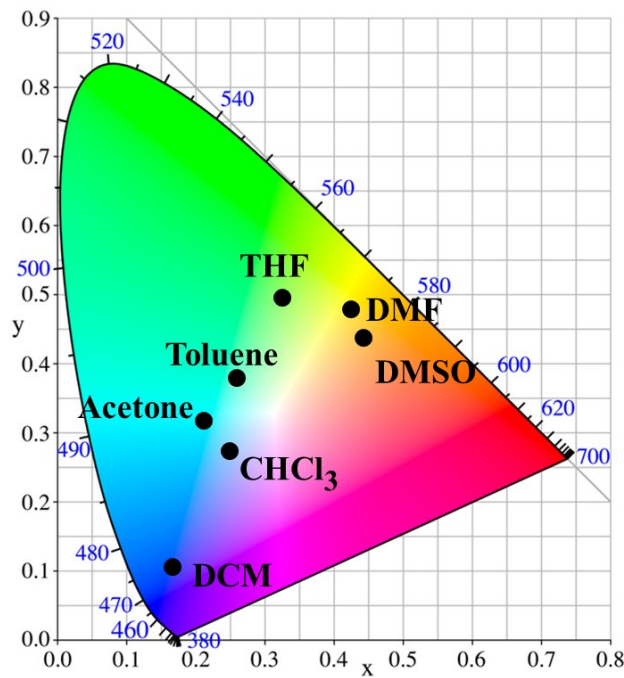


Figure S26 Corresponding CIE graph of complex **4** in different solvents (10^{-6} M) at room temperature.

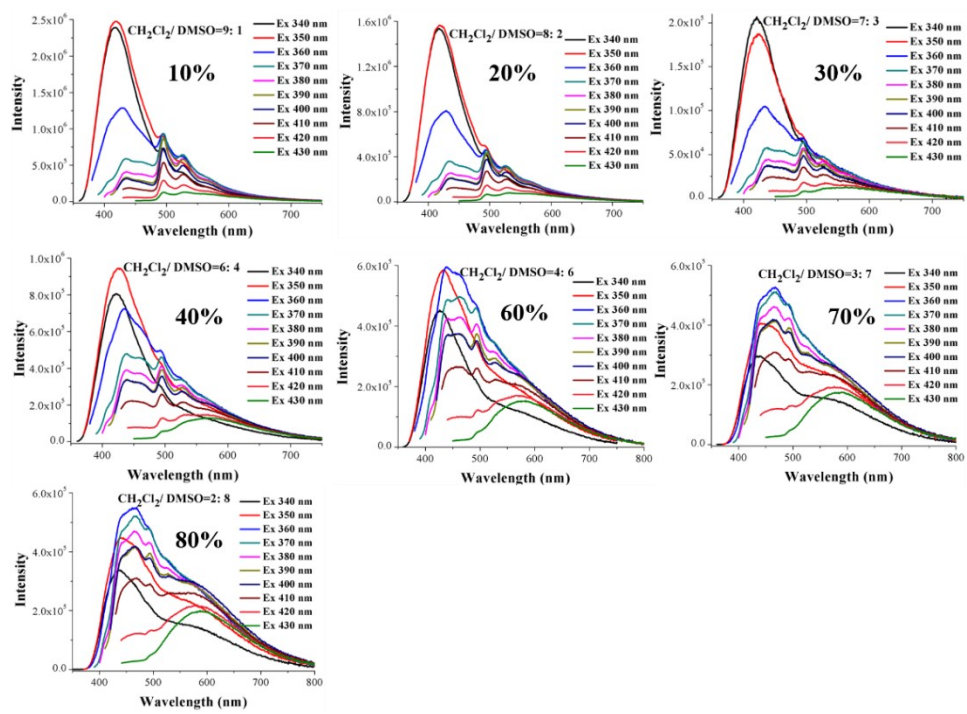


Figure S27 Emission spectra of complex **4** under the different ratio of DCM/ DMSO (10%–40% and 60%–80%) at the concentration of 10^{-5} M with different excitation bands.

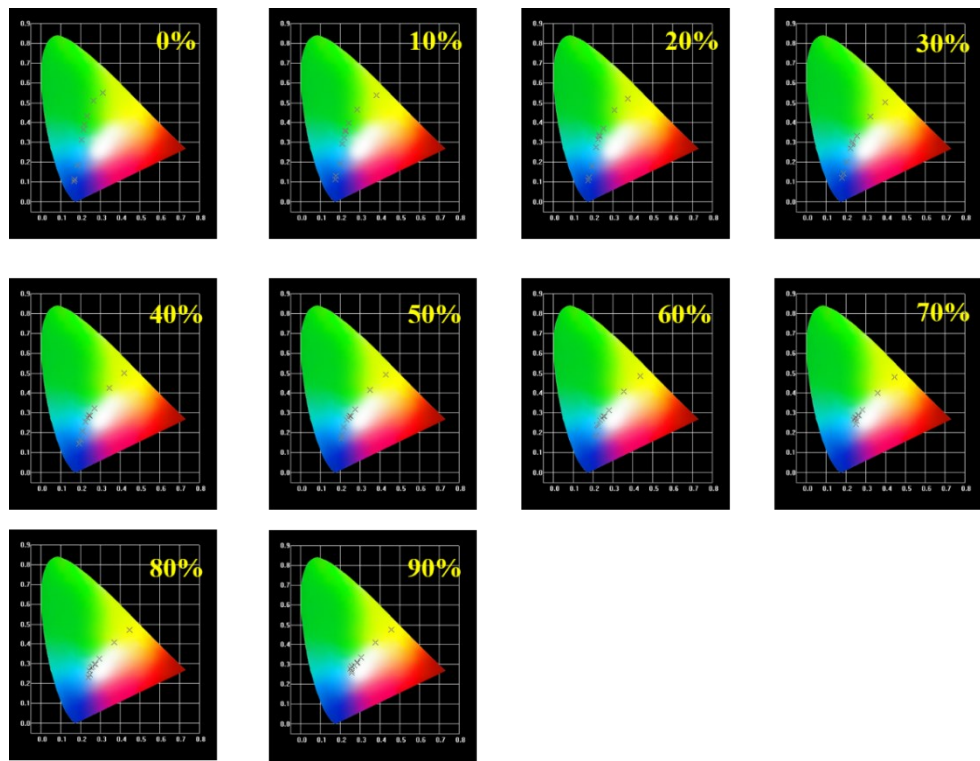


Figure S28 CIE graphs of complex **4** under the different ratio of DCM/DMSO (0%–90%) at the concentration of 10^{-5} M with different excitation bands.

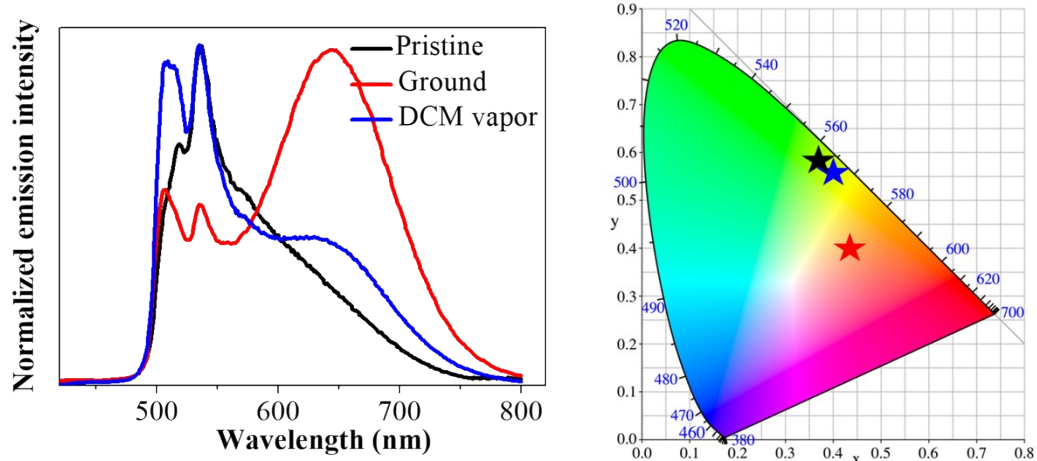


Figure S29 Normalized emission spectra of complex **1** in the pristine, ground and DCM vapor recycling solid state at room temperature.

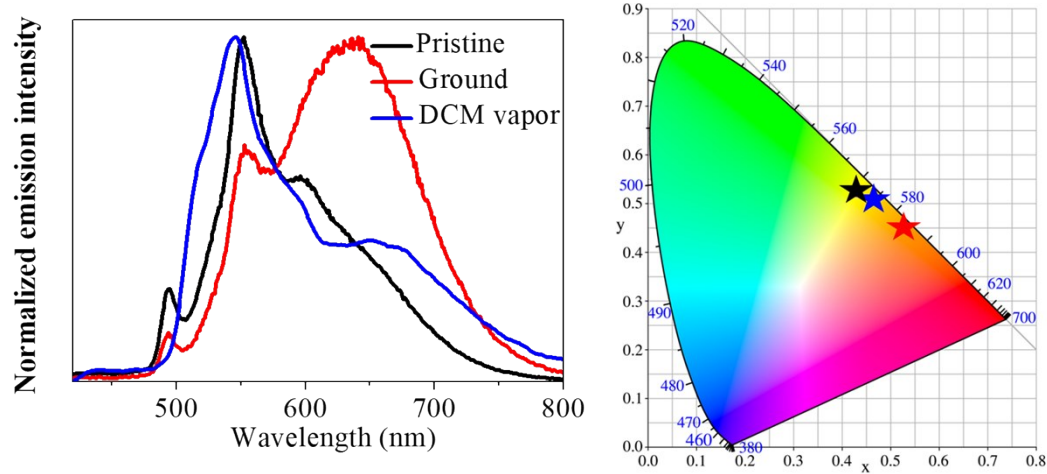


Figure S30 Normalized emission spectra of complex **2** in the pristine, ground and DCM vapor recycling solid state at room temperature.

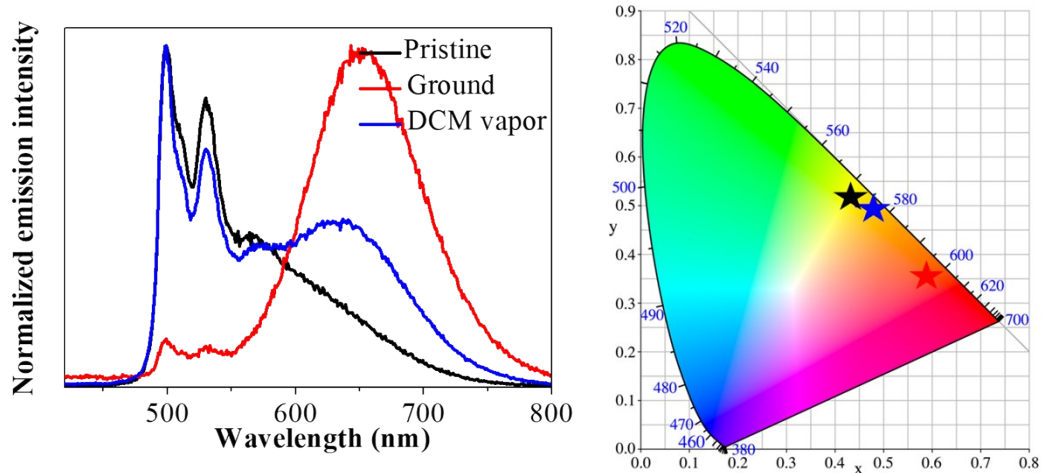


Figure S31 Normalized emission spectra of complex **3** in the pristine, ground and DCM vapor recycling solid state at room temperature.

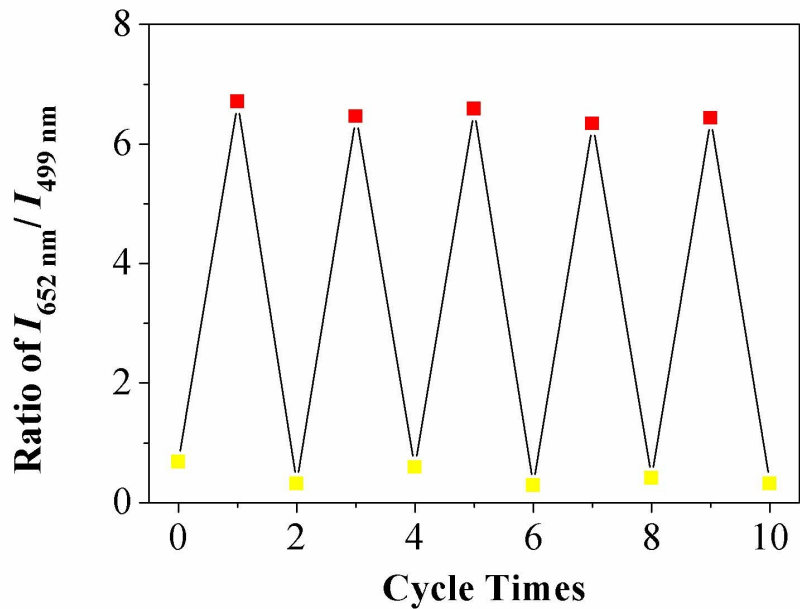


Figure S32 Cycle tests for reversible grinding–fuming of **3** ($\lambda_{\text{em max}} = 652 \text{ nm}$), ($\lambda_{\text{em max}} = 499 \text{ nm}$).

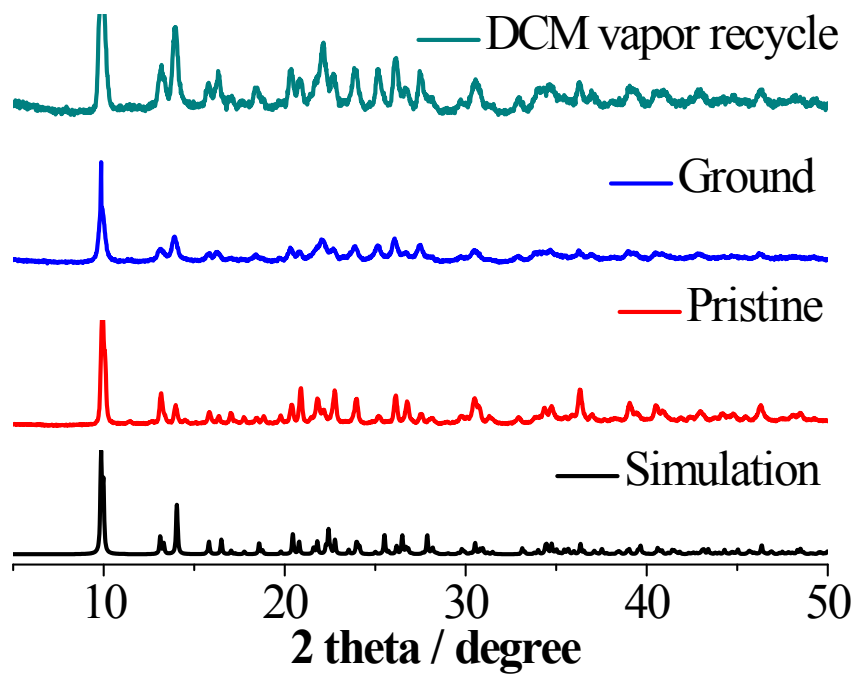


Figure S33 XRD pattern of complex 1 for the pristine, ground and vapor recycling in solid state at room temperature.

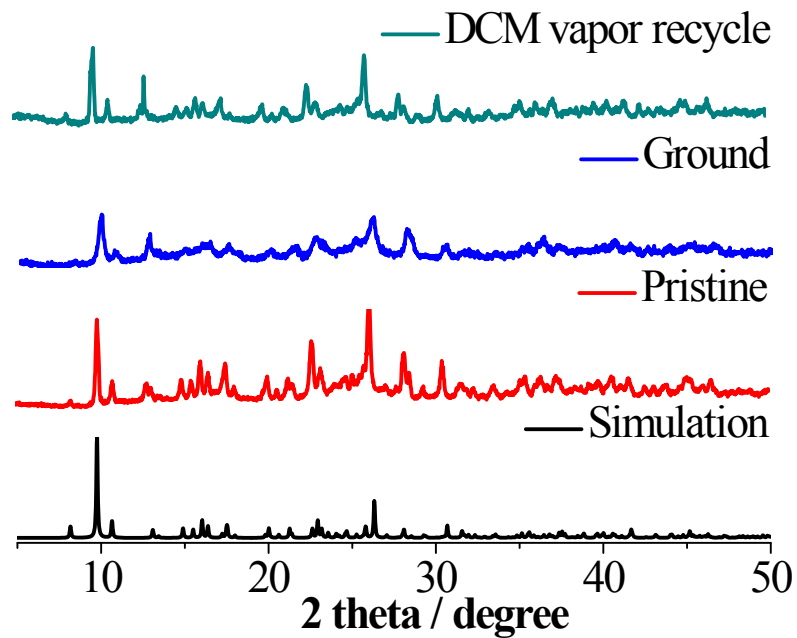


Figure S34 XRD pattern of complex 2 for the pristine, ground and vapor recycling in solid state at room temperature.

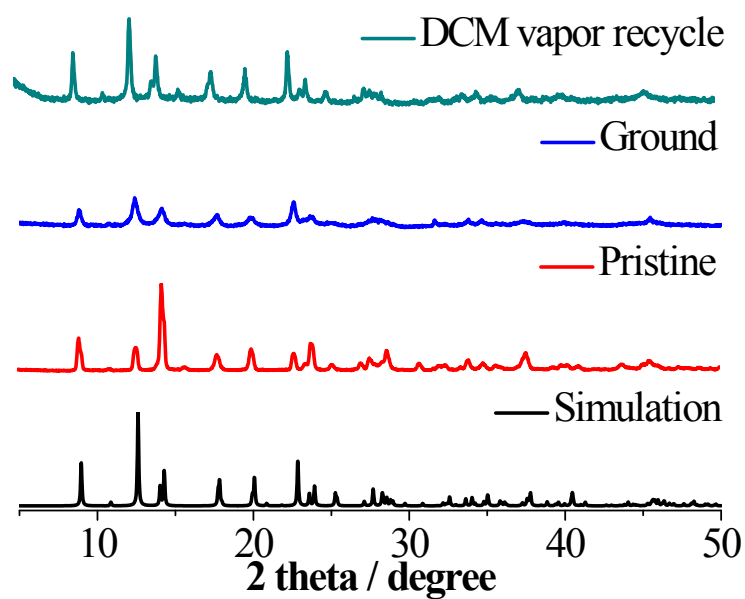


Figure S35 XRD pattern of complex 3 for the pristine, ground and vapor recycling in solid state at room temperature.

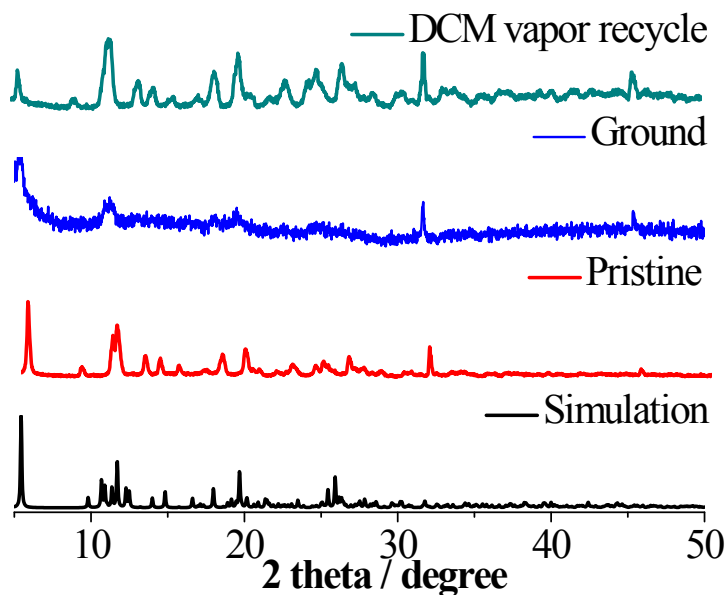


Figure S36 XRD pattern of complex 4 for the pristine, ground and vapor recycling in solid state at room temperature.

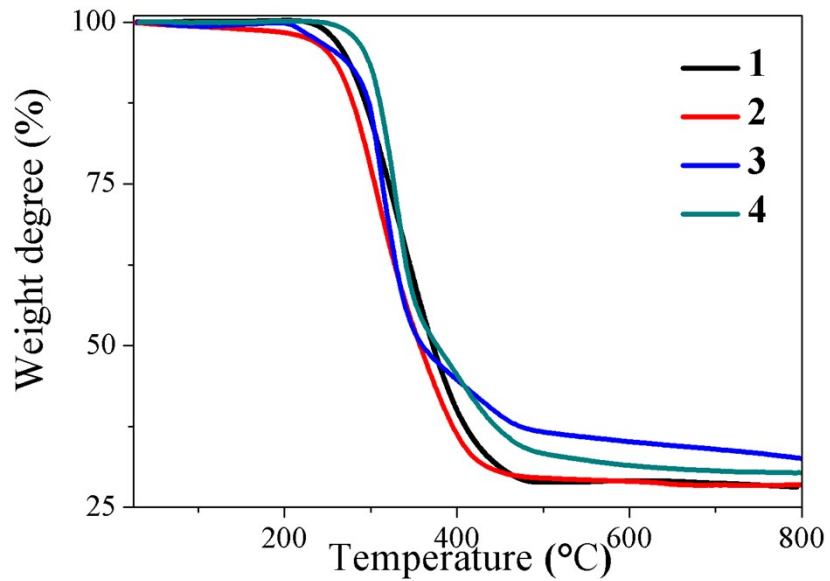


Figure S37 TG analysis of the complexes **1–4**.

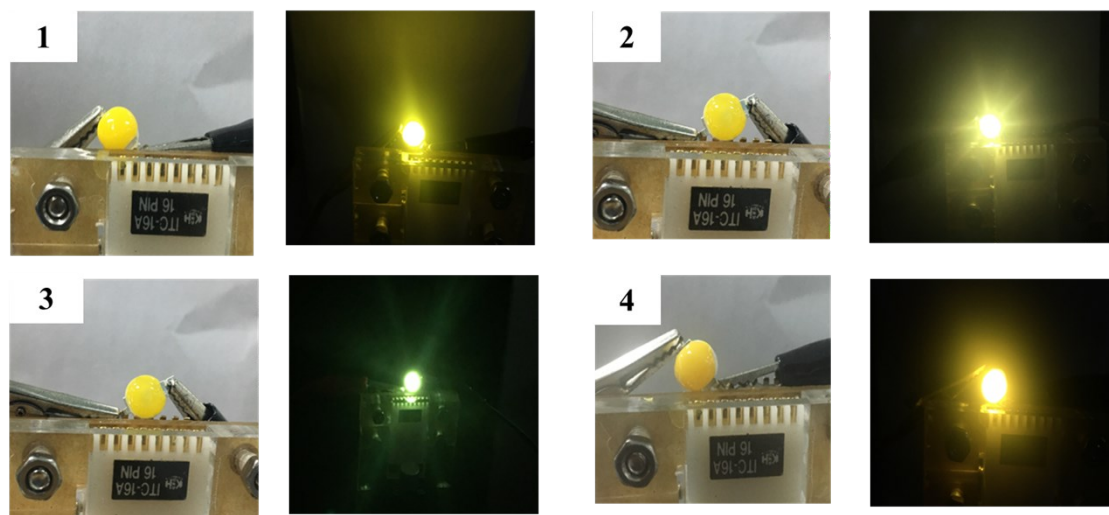


Figure S38 Photographs for turned on or not of coated LEDs of the platinum(II) complexes **1–4**.

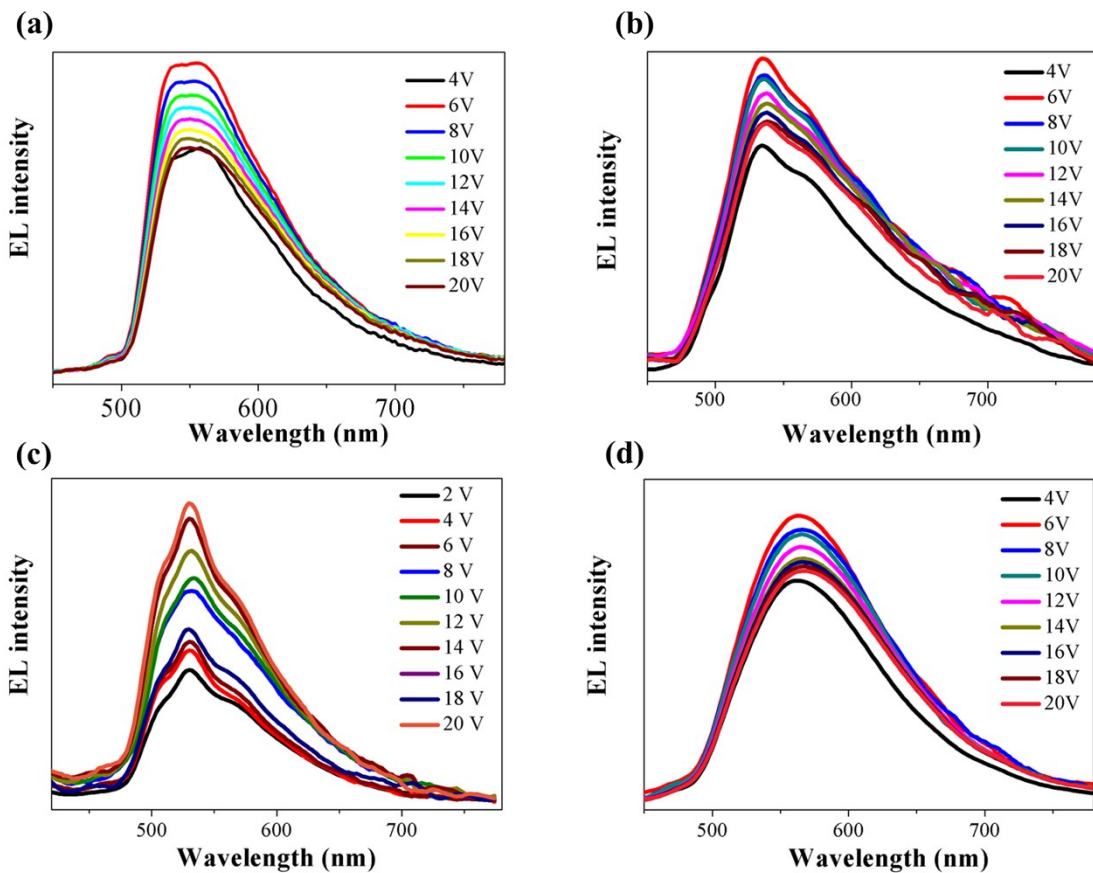


Figure S39 EL spectra of the complexes **1–4** at different voltages range from 2–20 V.

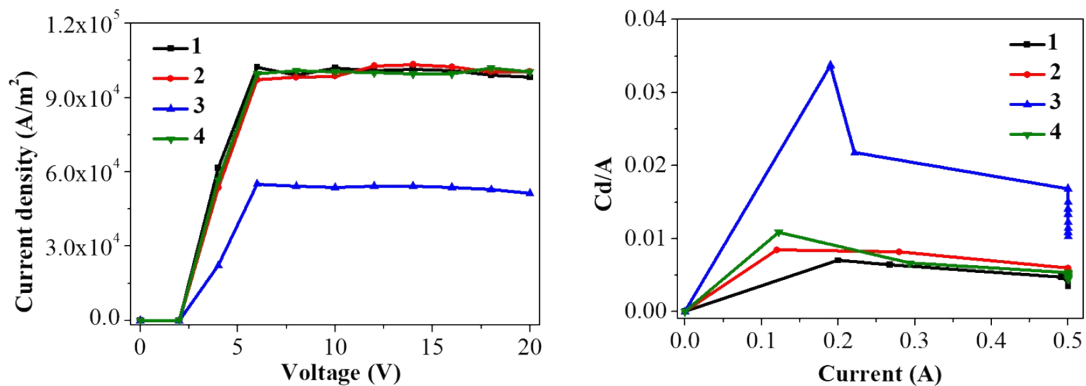


Figure S40 Current density curves of device **1–4** at voltage (0–20V); and luminous efficiency of the device.

Table S1 Crystal data and structure refinement for complexes **1–4**

Compound	1	2	3	4
Empirical formula	C ₁₈ H ₁₅ N ₂ ClPt	C ₁₇ H ₁₀ N ₃ ClPt	C ₂₆ H ₂₀ N ₂ Pt	C ₃₈ H ₂₉ N ₃ Pt
Formula weight	473.41	486.82	555.53	722.73
T/K	150(2)	150(2)	150(2)	150(2)
$\lambda/\text{\AA}$	1.54178	1.54184	1.54183	1.54184
Crystal system	monoclinic	orthorhombic	orthorhombic	triclinic
Space group	<i>P2₁/c</i>	<i>Pbca</i>	<i>Pmma</i>	<i>P-I</i>
<i>a</i> /\AA	8.10830(10)	16.6149(4)	9.9989(4)	9.1490(7)
<i>b</i> /\AA	10.3970(2)	7.8827(2)	12.4030(5)	10.3561(8)
<i>c</i> /\AA	18.1164(3)	21.6484(5)	16.2903(7)	16.9236(11)
$\alpha/^\circ$	90	90	90	73.883(6)
$\beta/^\circ$	102.212(2)	90	90	6.213(6)
$\gamma/^\circ$	90	90	90	65.045(7)
<i>V</i> /\AA ³	1492.69(4)	2835.30(12)	2020.26(14)	1394.2(2)
<i>Z</i>	4	8	2	2
$\rho/\text{g}\cdot\text{cm}^{-3}$	2.107	2.281	1.826	1.722
μ/mm^{-1}	17.652	20.229	6.960	9.662
<i>F</i> (000)	896	1824	1072	712
Data/restraints/parameters	2899/0 /199	2802/0/199	2837/460/273	5330/1/379
Quality-of-fit indicator	1.008	1.003	1.403	1.102
Final <i>R</i> indices [<i>I</i> > 2\sigma(<i>I</i>)]	<i>R</i> ₁ = 0.0704 <i>wR</i> ₂ = 0.1884	<i>R</i> ₁ = 0.0327 <i>wR</i> ₂ = 0.0763	<i>R</i> ₁ = 0.0722 <i>wR</i> ₂ = 0.2106	<i>R</i> ₁ = 0.0573 <i>wR</i> ₂ = 0.1476
<i>R</i> indices (all data)	<i>R</i> ₁ = 0.073 <i>wR</i> ₂ = 0.1927	<i>R</i> ₁ = 0.0394 <i>wR</i> ₂ = 0.0818	<i>R</i> ₁ = 0.0941 <i>wR</i> ₂ = 0.2180	<i>R</i> ₁ = 0.0713 <i>wR</i> ₂ = 0.1497

Table S2 Selected bond lengths (\AA) for complexes **1–4**

1	2	3	4
Pt(1)–C(13)	Pt(1)–C(5)	Pt(1)–C(6)	Pt(1)–C(13)
1.917(12)	1.894(6)	1.930(14)	1.955(9)
Pt(1)–Cl(5)	Pt(1)–Cl(1)	Pt(1)–C(7)	Pt(1)–C(19)
2.438(9)	2.4022(15)	2.045(18)	2.065(9)
Pt(1)–N(1)	Pt(1)–N(2)	Pt(1)–N(1)	Pt(1)–N(1)
2.017(10)	2.032(5)	2.004(14)	2.009(8)
Pt(1)–N(2)	Pt(1)–N(3)	Pt(1)–N(2)	Pt(1)–N(2)
2.011(9)	2.029(4)	2.018(13)	2.012(8)

Table S3 Selected bond angles ($^\circ$) for complexes **1–4**

1	2	3	4
C(13)–Pt–N(2)	C(5)–Pt–N(3)	C(7)–Pt–N(1)	C(13)–Pt(1)–N(1)
81.3(4)	81.0(2)	80.3(4)	79.6(3)
C(13)–Pt–N(1)	C(5)–Pt–N(2)	C(7)–Pt–N(2)	C(13)–Pt(1)–N(2)
81.1(5)	80.5(2)	80.3(4)	80.9(3)
N(2)–Pt–N(1)	N(3)–Pt–N(2)	N(1)–Pt–N(2)	N(1)–Pt(1)–N(2)
162.3(4)	161.54(19)	160.67(9)	160.4(3)
C(13)–Pt–Cl(1)	C(5)–Pt–Cl	C(6)–Pt–N(1)	N(1)–Pt(1)–C(19)
178.6(3)	177.91(16)	99.7(4)	99.2(3)
N(2)–Pt–Cl(1)	N(3)–Pt–Cl	C(6)–Pt–N(2)	N(2)–Pt(1)–C(19)
99.2(3)	99.10(14)	99.7(4)	100.3(3)
N(1)–Pt–Cl(1)	N(2)–Pt–Cl	C(7)–Pt–C(6)	C(13)–Pt(1)–C(19)
98.5(3)	99.36(14)	180	178.1(4)

Table S4 The photophysical data for complexes **1–4**

Medium T/K	Electronic absorption		Emission	QY [#]	
	λ_{max} [nm] (ϵ [$\text{dm}^3\text{mol}^{-1}\text{cm}^{-1}$]) (10^{-5})	λ_{em} [nm] (τ_0 [μs])	λ_{ex} (380)	χ^2	
1	DCM (298) Solid (298) Solid (77)	242 (34010), 266 (26150), 297 (17720), 328(7230), 348 (6920), 389 (5830) -	493, 526 (1.7) 568, 678 (0.23) 542, 684 (1.12)	0.017	1.16
	DCM (298)	225 (27940), 267 (36220), 312 (5870), 358 (8920), 377 (10780), 406 (11310)	480, 513 (2.2)	0.018	1.17
	Solid (298) Solid (77)	- -	540, 649 (0.31) 554, 688 (0.9)	0.016	-
2	DCM (298) Solid (298) Solid (77)	246(50500), 268 (60380), 297 (45360), 331 (9030), 342 (8040), 393 (9010) -	503, 532 (1.8) 523, 563 (0.65) 520, 580 (1.21) 640 (0.64)	0.011	1.17
	DCM (298)	247 (36820), 266 (39420), 300 (60800), 327 (40500), 397 (9020), 446 (4090)	528 (2.4), 569	0.009	1.10
	Solid (298) Solid (77)	- -	546, 687 (0.53) 541, 691 (1.11)	0.073	-
3	DCM (298) Solid (298) Solid (77)	- -	-	-	-
	DCM (298)	-	-	-	-
	Solid (298)	-	-	-	-
4	DCM (298) Solid (298) Solid (77)	- -	-	-	-
	DCM (298)	-	-	-	-
	Solid (298)	-	-	-	-

[-] Not measured. [#] The emission quantum yields were the maximum value under different excitation measured on a Hamamatsu C9920 -02G absolute PL quantum yield measurement system. χ^2 The value of "goodness-of-fit" parameter (chi-square).

Table S5 DFT calculation data about HOMO and LUMO energy of complexes **1–4** (#H→L assigned to the transition from HOMO to LUMO. The excitations and oscillator strength dependent on the calculated results. The oscillator strength of S₀→T₁ is 0, owing to the no consideration of intersystem crossing process in calculation.)

Complex	#Main configuration of S ₀ →S _n	#Main configuration of S ₀ →T _n
	^a excitation/nm	^a excitation/nm
	^b oscillator strength	
1	S ₀ →S ₁ : H→L (96.79)	S ₀ →T ₁ : H-4→L (2.57)
	^a 373.24	H-2→L+1 (6.18)
	^b 0.0093	H→L (81.74)
		H→L+1 (3.22)
		^a 508.36
	S ₀ →S ₂ : H→L+1 (94.33)	S ₀ →T ₂ : H-4→L+1 (5.89)
	H-2→L (2.11)	H-2→L (5.44)
	360.72	H-2→L+1 (2.87)
	^b 0.0587	H→L (4.63)
		H→L+1 (78.48)
2		^a 470.39
	S ₀ →S ₃ : H-1→L (93.76)	S ₀ →T ₃ : H-5→L+1 (2.55)
	329.56	H-5→L+2 (2.89)
	^b 0.0008	H-4→L (4.06)
		H-2→L (22.16)
		H-2→L+1 (47.85)
		H→L (9.79)
		^a 448.48
	S ₀ →S ₁ : H-2→L (63.85)	S ₀ →T ₁ : H-6→L (2.17)
	H-2→L+1(33.28)	H-3→L (3.10)
2	354.69	H→L (54.04)
	^b 0.0182	H→L+1 (32.06)
		H→L+3 (2.10)
		^a 488.99

	$S_0 \rightarrow S_2:$ H-4→L (63.55) H-3→L+1 H→L+2 333.25 ^b 0.0248	$S_0 \rightarrow T_2:$ H-4→L (3.48) H→L (59.48) H→L+1 (31.24) ^a 476.98
	$S_0 \rightarrow S_1:$ H→L (92.39) ^a 359.43 ^b 0.0059	$S_0 \rightarrow T_1:$ H-4→L (2.06) H-2→L+1 (3.06) H-1→L (32.53) H→L (58.45) ^a 515.14
3	$S_0 \rightarrow S_2:$ H-1→L (97.83) H→L+1 ^a 327.86 ^b 0.0321	$S_0 \rightarrow T_2:$ H-2→L+1 (5.62) H-1→L (49.11) H→L (39.43) ^a 489.05
	$S_0 \rightarrow S_3:$ H-2→L+1 (97.30) H-1→L+1 ^a 305.24 ^b 0.1470	$S_0 \rightarrow T_3:$ H-4→L+1 (5.79) H-1→L+1 (42.56) H→L+1 (49.12) ^a 488.87
	$S_0 \rightarrow S_4:$ H-2→L+1 (60.84) H→L+2 ^a 294.22 ^b 0.0971	$S_0 \rightarrow T_4:$ H-4→L+1 (2.55) H-1→L+1 (44.92) H-2→L+1 (49.36) ^a 462.82
4	$S_0 \rightarrow S_1:$ H-2→L (2.23) H-1→L (87.60) H→L (8.60) ^a 448.78 ^b 0.0283	$S_0 \rightarrow T_1:$ H-1→L (30.43) H→L (63.57) ^a 559.03

$S_0 \rightarrow S_2:$	$S_0 \rightarrow T_2:$
H-2→L (5.36)	H-4→L+1 (2.54)
H-2→L+1 (4.59)	H-1→L+1 (24.44)
H-1→L+1 (79.33)	H→L+1 (68.52)
H→L+1 (8.36)	^a 507.44
^a 427.42	
^b 0.0255	
$S_0 \rightarrow S_3:$	$S_0 \rightarrow T_3:$
H-2→L (89.55)	H-4→L (7.27)
H-1→L+1 (5.20)	H-3→L+1 (17.64)
^a 327.63	H-2→L (18.90)
^b 0.0340	H-1→L (22.55)
	H→L (22.97)
	^a 486.78
$S_0 \rightarrow S_4:$	$S_0 \rightarrow T_4:$
H-2→L (89.55)	H-3→L+1 (36.35)
H-1→L+1 (5.20)	H-2→L+1 (8.23)
^a 299.56	H-1→L (20.73)
^b 0.0685	H→L (7.37)
	H→L+1 (6.39)
	^a 459.11

Table S6 Molecular orbital (MO) compositions of complexes **1–4** based on the optimized S_0 states.

Complex	MO	Pt(%)	N^C^N units	Alkynyl ligands
1	LUMO	2.63	93.09	/
	HOMO	23.46	67.01	/
2	LUMO	2.55	95.22	/
	HOMO	21.35	70.21	/
3	LUMO	1.25	92.07	2.78
	HOMO	25.9	3.17	68.49
4	LUMO	1.39	91.83	1.02
	HOMO	26.34	0.89	66.38

Table S7 Cartesian coordinates of the optimized ground-state geometry for complex **1**

Pt	2.54920000	3.04540000	14.08020000
Cl	0.18080000	2.97350000	14.48130000
N	9.65820000	3.41720000	12.88730000
N	2.55700000	4.06510000	12.32010000
N	3.18510000	2.04240000	15.72760000
C	8.54170000	3.39430000	13.14710000
C	7.12110000	3.35010000	13.41980000
C	6.65430000	2.69430000	14.57800000
H	7.24410000	2.33560000	15.20150000
C	5.27020000	2.60440000	14.75340000
C	4.42120000	3.16730000	13.79650000
C	4.90140000	3.80420000	12.63620000
C	6.26880000	3.89640000	12.44780000
H	6.61610000	4.31100000	11.69010000
C	3.79480000	4.29210000	11.79190000
C	3.94940000	4.91570000	10.57960000
H	4.80000000	5.05600000	10.23100000
C	2.84110000	5.33030000	9.88250000
H	2.93590000	5.73620000	9.05120000
C	1.58340000	5.14030000	10.42370000
H	0.82410000	5.43430000	9.97560000

C	1.47870000	4.50020000	11.65550000
H	0.63640000	4.37100000	12.02570000
C	4.53420000	1.95180000	15.85750000
C	5.11910000	1.26360000	16.92260000
H	6.04450000	1.20680000	17.00700000
C	4.28500000	0.67160000	17.84040000
H	4.65050000	0.19470000	18.55050000
C	2.92420000	0.77250000	17.72790000
H	2.36430000	0.38390000	18.36000000
C	2.40250000	1.46780000	16.64760000
H	1.48040000	1.53630000	16.56100000

Table S8 Cartesian coordinates of the optimized ground-state geometry for complex 2

Pt	2.54920000	3.04540000	14.08020000
Cl	0.18080000	2.97350000	14.48130000
N	9.65820000	3.41720000	12.88730000
N	2.55700000	4.06510000	12.32010000
N	3.18510000	2.04240000	15.72760000
C	8.54170000	3.39430000	13.14710000
C	7.12110000	3.35010000	13.41980000
C	6.65430000	2.69430000	14.57800000
H	7.24410000	2.33560000	15.20150000

C	5.27020000	2.60440000	14.75340000
C	4.42120000	3.16730000	13.79650000
C	4.90140000	3.80420000	12.63620000
C	6.26880000	3.89640000	12.44780000
H	6.61610000	4.31100000	11.69010000
C	3.79480000	4.29210000	11.79190000
C	3.94940000	4.91570000	10.57960000
H	4.80000000	5.05600000	10.23100000
C	2.84110000	5.33030000	9.88250000
H	2.93590000	5.73620000	9.05120000
C	1.58340000	5.14030000	10.42370000
H	0.82410000	5.43430000	9.97560000
C	1.47870000	4.50020000	11.65550000
H	0.63640000	4.37100000	12.02570000
C	4.53420000	1.95180000	15.85750000
C	5.11910000	1.26360000	16.92260000
H	6.04450000	1.20680000	17.00700000
C	4.28500000	0.67160000	17.84040000
H	4.65050000	0.19470000	18.55050000
C	2.92420000	0.77250000	17.72790000
H	2.36430000	0.38390000	18.36000000
C	2.40250000	1.46780000	16.64760000

H	1.48040000	1.53630000	16.56100000
---	------------	------------	-------------

Table S9 Cartesian coordinates of the optimized ground-state geometry for complex **3**

Pt	0.06838100	0.00001600	0.00001300
N	0.41684900	-2.02429900	-0.02154600
N	0.41692900	2.02431700	0.02163400
C	-0.55104900	-2.95558200	-0.03298000
H	-1.56192500	-2.56294500	-0.03018700
C	-0.27060000	-4.31647700	-0.04731200
H	-1.08238300	-5.03482700	-0.05634200
C	1.06451800	-4.71186200	-0.04973200
H	1.32950100	-5.76499900	-0.06068200
C	2.06927000	-3.74810800	-0.03829500
H	3.10160000	-4.06116300	-0.04046400
C	1.75302900	-2.38208600	-0.02427500
C	2.69500600	-1.24213800	-0.01221400
C	4.10977200	-1.24542900	-0.01210200
C	4.97530200	-2.48377000	-0.02371600
H	4.79780900	-3.11585600	0.85429100
H	4.79894500	-3.09869400	-0.91406900
H	6.03352100	-2.21095300	-0.02041500
C	4.75620200	-0.00007400	-0.00024400

H	5.84329200	-0.00009400	-0.00037800
C	4.97539800	2.48361600	0.02310200
H	6.03360500	2.21076500	0.01920700
H	4.79746600	3.11584900	-0.85470500
H	4.79953300	3.09840300	0.91365200
C	4.10982000	1.24530500	0.01174500
C	2.69505500	1.24206400	0.01216300
C	2.03116900	-0.00002500	0.00001400
C	1.75312400	2.38204700	0.02441500
C	2.06942700	3.74805200	0.03876000
H	3.10177200	4.06105700	0.04108500
C	1.06471700	4.71184800	0.05036900
H	1.32974600	5.76497000	0.06157600
C	-0.27041800	4.31652100	0.04781200
H	-1.08216900	5.03490500	0.05695900
C	-0.55092700	2.95564100	0.03322400
H	-1.56182000	2.56304700	0.03035400
C	-3.22355600	0.00004600	-0.00004500
C	-1.99358900	0.00005800	-0.00002800
C	-4.65123500	0.00004400	-0.00008700
C	-5.37868200	0.29790700	-1.17250300
C	-5.37875200	-0.29783400	1.17228300

C	-6.77148100	0.29675900	-1.16924200
H	-4.83199200	0.52756800	-2.08198900
C	-6.77155100	-0.29670600	1.16893400
H	-4.83211600	-0.52749200	2.08180200
C	-7.47684500	0.00002300	-0.00017600
H	-7.30999800	0.52854000	-2.08457200
H	-7.31012200	-0.52849700	2.08422900
H	-8.56321200	0.00001500	-0.00021000

Table S10 Cartesian coordinates of the optimized ground-state geometry for complex 4

Pt	-2.58391500	0.00873700	-0.07961500
N	-2.84730700	-1.94968300	0.28089200
N	-2.99728300	1.96050600	-0.33762600
N	6.36789100	0.00089200	-0.02407800
C	-1.84659200	-2.84142000	0.48354200
H	-0.96738400	-2.54476100	0.42997800
C	-2.07904900	-4.16877500	0.76645300
H	-1.36630300	-4.75795700	0.86600000
C	-3.37032200	-4.61790000	0.90068800
H	-3.56461900	-5.50754200	1.08929900
C	-4.22297000	-3.80126500	0.76156100
H	-5.08570500	-4.12267000	0.89567200

C	-4.15499400	-2.36830100	0.41291400
C	-5.13477600	-1.25959600	0.20133400
C	-6.55488800	-1.34390900	0.20580900
C	-7.54344200	-2.52529500	0.26475200
H	-7.05586500	-3.34781000	0.35316900
H	-8.12747800	-2.41763500	1.01915700
H	-8.06491700	-2.54740600	-0.54096600
C	-7.23505200	-0.13313500	0.07747100
H	-8.16339800	-0.16463100	0.09604200
C	-6.63820300	1.13114200	-0.07672700
C	-7.55330000	2.33066900	-0.16648000
H	-8.46566300	2.04248500	-0.09874400
H	-7.35484900	2.93821900	0.55016800
H	-7.41817400	2.77378400	-1.00735300
C	-5.25080500	1.16462800	-0.13616200
C	-4.53536900	-0.07260600	0.01454600
C	-4.32740200	2.30609500	-0.33119600
C	-4.69708500	3.65220400	-0.45931100
H	-5.59830700	3.88633300	-0.46182600
C	-3.72610000	4.63408500	-0.58216500
H	-3.97460900	5.52599900	-0.66108600
C	-2.38917900	4.28832400	-0.58681400

H	-1.72883400	4.93703000	-0.67365700
C	-2.05744700	2.93825800	-0.45821200
H	-1.16003500	2.69627100	-0.45492900
C	-0.52559600	0.04470600	-0.22384500
C	0.69102300	0.00861200	-0.28118700
C	2.12959500	-0.02171500	-0.26535700
C	2.80335200	-0.82201200	0.64389900
H	2.31178200	-1.37995800	1.20242400
C	4.18207600	-0.81851200	0.75067200
H	4.60420700	-1.33901300	1.39439100
C	4.93029100	-0.02884300	-0.11319400
C	4.28603600	0.73660400	-1.07475200
H	4.78509600	1.23048500	-1.68480500
C	2.90970100	0.76873000	-1.13090100
H	2.48868400	1.32059200	-1.75004000
C	7.13012900	-1.11257700	-0.40093300
C	6.56422000	-2.15939500	-1.12602900
H	5.67288000	-2.09726500	-1.38403000
C	7.28336500	-3.28933700	-1.47541600
H	6.87092300	-3.97676400	-1.94767700
C	8.62952300	-3.39248700	-1.11779600
H	9.12759600	-4.13805600	-1.36451900

C	9.20121100	-2.37411100	-0.39561100
H	10.09527000	-2.43972200	-0.14879400
C	8.47739500	-1.25045100	-0.02630000
H	8.88825000	-0.58200300	0.47423100
C	6.95238600	1.20031000	0.47474100
C	7.99709800	1.79381000	-0.19096700
H	8.33430600	1.40130500	-0.96386200
C	8.56086400	2.99134400	0.28962000
H	9.24837000	3.40220600	-0.18300600
C	8.09451000	3.56075600	1.46058900
H	8.49766200	4.32413000	1.80780800
C	7.00822500	2.96962700	2.11648100
H	6.65293100	3.36720100	2.87892400
C	6.45389400	1.77797900	1.62276800
H	5.74656000	1.37619000	2.07278300

References

1. G. Sheldrick, J Acta Crystallographica Section A, 2008, **64**, 112-122.
2. O. V. Dolomanov, L. J. Bourhis, R. J. Gildea, J. A. K. Howard and H. Puschmann, *J. Appl. Crystallogr.*, 2009, **42**, 339-341.
3. X. Gao, S. Bai, D. Fazzi, T. Niehaus, M. Barbatti and W. Thiel, *J. Chem. Theory Comput.*, 2017, **13**, 515-524.
4. K. Y. Suponitsky, S. Tafur and A. E. Masunov, *J. Chem. Phys.*, 2008, **129**, 044109.
5. J. A. G. Williams, AndrewBeeby, E. S. Davies, J. A. Weinstein and C. Wilson, *Inorg. Chem.*, 2003, **42**, 8609-8611.
6. A. Y.-Y. Tam, D. P.-K. Tsang, M.-Y. Chan, N. Zhu and V. W.-W. Yam, *Chem. Commun.*, 2011, **47**, 3383-3385.
7. J. Kuwabara, K. Yamaguchi, K. Yamawaki, T. Yasuda, Y. Nishimura and T. Kanbara, *Inorg. Chem.*, 2017, **56**, 8726-8729.
8. B. Schulze, C. Fribe, M. Jäger, H. Görls, E. Birckner, A. Winter and U. S. Schubert, *Organometallics*, 2017, **37**, 145-155.